X-ray emission spectra induced by hydrogenic ions in charge transfer collisions

Matthew Rigazio, V. Kharchenko, and A. Dalgarno
Institute for Theoretical Atomic and Molecular Physics, Harvard-Smithsonian Center for Astrophysics, Cambridge, Massachusetts 02138
(Received 7 February 2002; published 2 December 2002)

Theoretical models are constructed of the hard x-ray spectra resulting from electron capture by fully stripped Ne^{10+} ions traversing the gases Ne, He, H_2, CO_2, and H_2O. The measured spectra are superpositions of individual lines of Ne^{9+}. An exact description of the radiative cascade is used. Initial excited populations that reproduce the measured spectra are derived and quantitative predictions of the energies and intensities of lines in the soft x-ray and extreme ultraviolet regions are made. These lines when observed will be powerful diagnostic probes of the capture mechanism and of the diverse range of laboratory and astrophysical plasmas in which it occurs.

DOI: 10.1103/PhysRevA.66.064701 PACS number(s): 34.70.+e, 52.70.La

The discovery that comets emit x rays and extreme ultraviolet (EUV) radiation [1–10] has generated several suggestions for the possible excitation mechanisms, of which bremsstrahlung [10–13] and electron capture by solar wind ions [14] are the most plausible. The detection of structure in the spectra [9,10] strongly indicated that electron capture by highly charged heavy ions of the solar wind colliding with the cometary atmosphere was a major source, although bremsstrahlung may be contributing also. Calculations of the spectra resulting from charge transfer for typical solar wind ion compositions have been carried out by Häberli *et al.* [15], Wegmann *et al.* [16], Schwadron and Cravens [17], and Kharchenko and Dalgarno [18,19]. The models predict multiple emission lines with specific relative intensities. The more comprehensive calculations of Kharchenko and Dalgarno [18] predict ratios for the intensities of spectral features at 400 eV, 560 eV, and 670 eV of 2.2:3.2:1.0, whereas Lisse *et al.* [10] report for comet C/Linear 1999 S4 ratios of 2.3:4.5:1.0. The spectral features consist of several unresolved emission lines. A small adjustment in the adopted solar wind ion composition would bring the theoretical and measured spectra into agreement. The calculations demonstrate that if sufficient accuracy and spectral resolution can be achieved cometary spectra will be a powerful diagnostic probe of the solar wind ion composition [15,17–19].

Laboratory experiments [20–27] on x rays produced by specific ions in individual gases in conjunction with cross section calculations [26–34] open the way to a reliable quantitative description of the electron capture process and its application to comets, the planets Earth [35,36] and Jupiter [37–40], the soft x-ray background [41,42], astrophysical environments where gamma-ray lines have been observed [43,44], high temperature plasmas [45–47], and possibly main sequence stellar winds [48].

In this Brief Report we analyze the measurements of x rays induced by fully stripped ions colliding with various gases [23,24]. The process may be represented by

$$X^{m+} + A \rightarrow X^{(m-1)+}(nl) + A^+, \tag{1}$$

where A is the target gas atom or molecule and $X^{(m-1)+}(nl)$ is the excited state of the hydrogenic ion with principal quantum number n and azimuthal quantum number l. Following the initial capture processes the $\{nl\}$ states cascade through the lower lying energy levels by a complicated series of radiative transitions, giving rise to numerous emission lines in the x-ray and EUV regions with specific relative intensities. The radiative transitions are subject to the selection rule that $\Delta l = \pm 1$ and the spectra are sensitive to the initial l populations. To calculate the transition probabilities $A(n'l',nl)$ from state nl to state $n'l'$ and the related branching ratios $p_{n'l',nl} = A(n'l',nl)/\Sigma_{n'l'} A(n'l',nl)$, we used exact nonrelativistic formulas [49,50]. The solution of the cascading problem was obtained using the formulation of Kharchenko *et al.* [40]. Given an initial $\{nl\}$ distribution we get an exact representation of the resulting spectrum.

The numbers of cascading photons $\eta^{nl}_{n'l'}$ emitted by an excited ion in $nl \rightarrow n'l'$ transitions are calculated taking into account all possible pathways of the photon cascade relaxation. It is convenient to describe excited states of hydro-

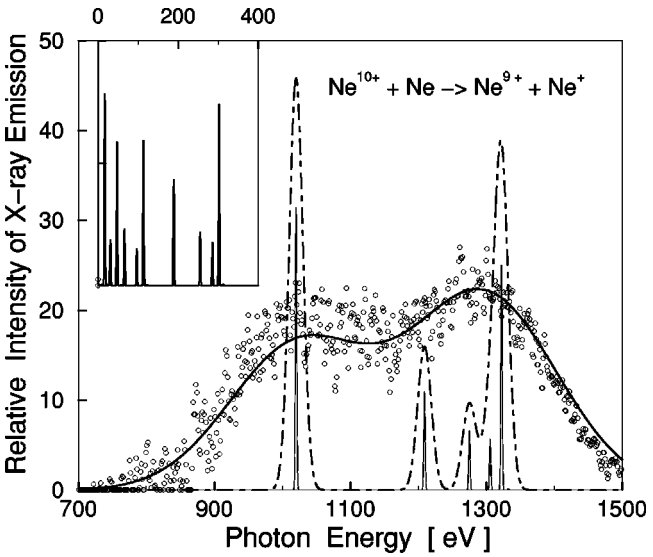

FIG. 1. X-ray emission spectra induced in $Ne^{10+} + Ne$ collisions. Experimental data by Beiersdorfer *et al.* [21] are shown by circles. The Ne^{*9+} emission spectra calculated for different photon energy resolutions Γ are shown by the thin solid curve for a spectral resolution of 1 eV, by the dot-dashed curve for $\Gamma = 10$ eV, and by the thick solid curve for $\Gamma = 100$ eV.

 ©2002 The American Physical Society

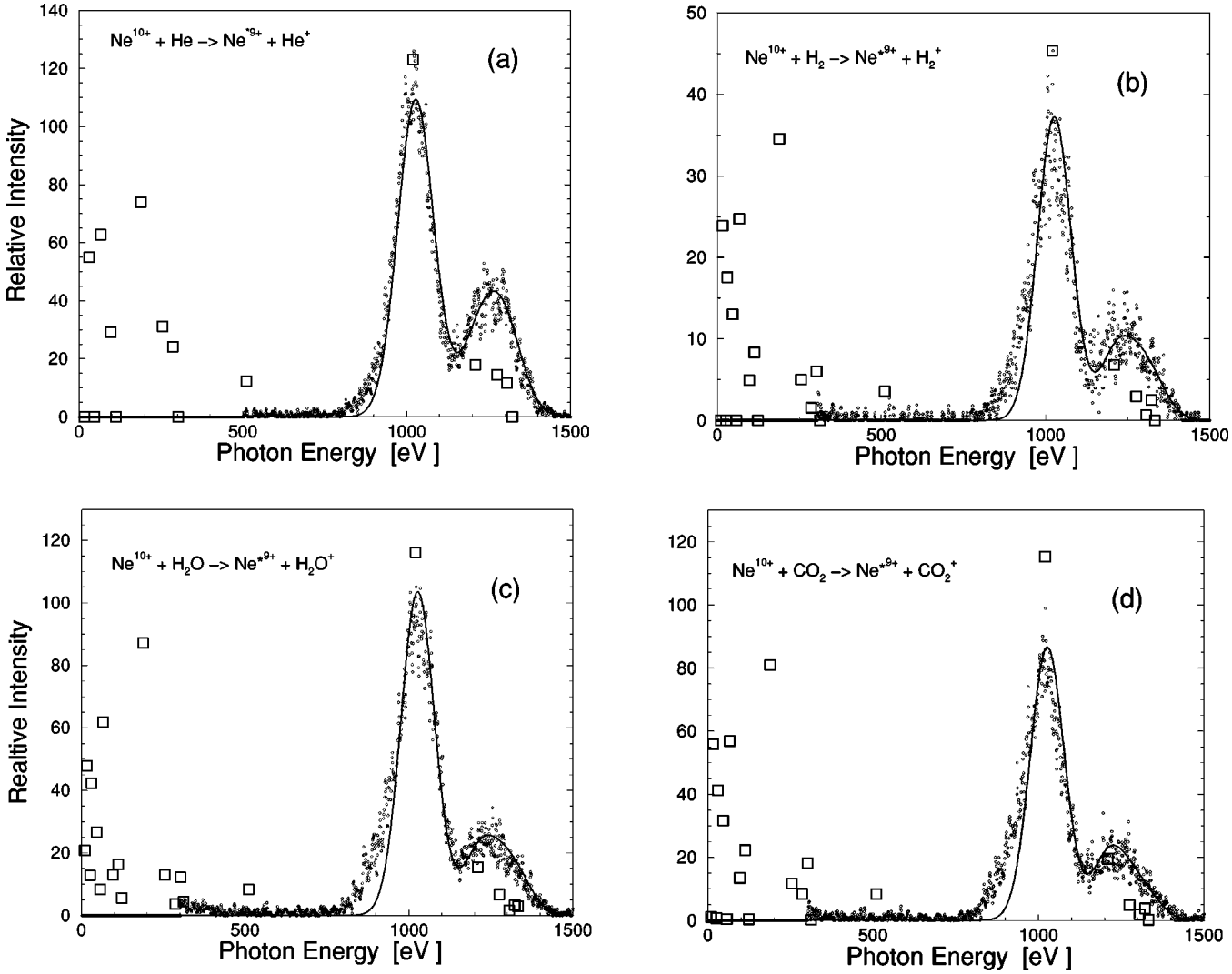

FIG. 2. X-ray emission spectra induced in Ne^{10+} collisions with He atoms and with H_2, H_2O, and CO_2 molecules. Experimental data by Greenwood *et al.* [20] are shown by circles. The Ne^{*9+} emission spectra calculated for a photon energy resolution of 50 eV are shown by the solid curves. The relative intensities of $n \rightarrow n'$ cascading transitions are shown by squares.

genic ions by the index number $N=n(n-1)/2+l+1$, which represents the pair of quantal numbers $\{n,l\}$. The branching ratios $p_{n'l',nl}$ of $N(n,l) \rightarrow N'(n',l')$ transitions compose the transition matrix $\hat{\mathbf{P}}=\{P_{N',N}\}=\{p_{n'l',nl}\}$. The initial populations of different excited states in single electron capture collisions are given by the vector $\mathbf{C}[0]=\{c_N(0)\}$ normalized to unity. The vector components $c_N(0)$ are the probabilities of electron capture into $N(n,l)$ excited states: $c_N(0) = \sigma(n,l)/\sigma$, where $\sigma(nl)$ and σ are the partial and total electron capture cross sections. The population of the excited electronic states is altered due to radiative cascading. After emission of the first photon the new occupation numbers of excited states are given by the vector $\mathbf{C}[1]=\hat{\mathbf{P}}\mathbf{C}[0]$, after a second photon emission by $\mathbf{C}[2]=\hat{\mathbf{P}}\mathbf{C}[1]=\hat{\mathbf{P}}^2\mathbf{C}[0]$, and so on. Each multiplication by the transition matrix $\hat{\mathbf{P}}$ clears the level with the highest occupied principal quantum number n. The populations of all excited states are terminated after i_m cascading steps, where i_m is the number of intermediate excited states in the longest relaxation path. The maximum number of photons emitted in the relaxation pathways depends on the ion excess charge q and on the target ionization potential.

The fraction of photons $\eta^{nl}_{n'l'}$ emitted in $N \rightarrow N'$ transitions is calculated as

$$\eta^{nl}_{n'l'} = p_{n'l',nl}(\mathbf{C}[0]+\mathbf{C}[1]+\mathbf{C}[2]+\cdots)_{N(n,l)} = p_{n'l',nl}(\mathbf{C}_{\mathrm{tot}})_{N(n,l)}, \quad (2)$$

where $\mathbf{C}_{\mathrm{tot}}$ is the vector of the total population via all possible cascading pathways calculated as

$$\mathbf{C}_{\mathrm{tot}} = \sum_{i=0}^{i_m} \hat{\mathbf{P}}^i \cdot \mathbf{C}[0]. \quad (3)$$

The initial populations depend on the nature of the colliding systems and on the projectile ion velocity. In Fig. 1 recent measurements of x-ray emission spectra in $Ne^{10+}+Ne$ collisions [24] at energy of (9 ± 4) eV amu^{-1} are compared

TABLE I. Relative intensities of Ne^{*9+} emission lines.

	$6p$-$1s$	$5p$-$1s$	$4p$-$1s$	$3p$-$1s$	$2p$-$1s$	$3d$-$2p$	$4f$-$3d$	$5g$-$4f$	$6h$-$5g$	$6g$-$4f$	$6g$-$5f$	$6f$-$3d$	$6d$-$2p$	$4d$-$2p$	$5f$-$3d$
$\hbar\omega$ (eV)	1324	1308	1277	1211	1022	189	66.1	30.6	16.6	47.2	16.6	113	302	255	96.8
He		0.095	0.12	0.15	1	0.57	0.41	0.32						0.20	0.16
H_2	0.056	0.014	0.065	0.15	1	0.74	0.51	0.33	0.32	0.18	0.15	0.13	0.11	0.10	0.10
H_2O	0.028	0.014	0.058	0.13	1	0.73	0.49	0.30	0.25	0.15	0.12	0.098	0.086	0.10	0.10
CO_2	0.033	0.017	0.041	0.17	1	0.68	0.46	0.30	0.29	0.16	0.13	0.13	0.13	0.094	0.086

with theoretical spectra calculated by applying our photon cascading scheme to the initial nl distribution from a multicrossing Landau-Zener model. The theoretical spectra are given for photon energy resolutions of 1, 10, and 100 eV. The low resolution spectra are in very good agreement with the experimental data and the earlier disagreement with the theoretical models [15,16] is removed by our more accurate description of the cascading. The predicted spectra of the soft cascading photons are shown in the inset of Fig. 1. The figure demonstrates the substantial enhancement in diagnostic capability provided by high spectral resolution and by the detection of cascading photons.

In Figs. 2(a)–2(d) we reproduce the measurements of Greenwood *et al.* [23] of the x-ray spectra resulting from collisions of fully stripped Ne^{10+} ions traversing gases of He, H_2, H_2O, and CO_2 at energies of 3 keV/amu with a spectral resolution of 100 eV. Each spectrum has two main peaks centered at 1.3 keV and 1.0 keV. Greenwood *et al.* interpreted the spectra as a superposition of the α, β, γ, and δ lines of the Lyman series of Ne^{9+}.

Theoretical studies of charge transfer [30,32–34,51] indicate that capture occurs preferentially into levels with a narrow range of principal quantum numbers n. The distribution of orbital angular momentum l states depends sensitively on the projectile velocity, changing from an approximately statistical distribution at high energies to small values of l at low energies [23,30,51]. We use these model features for an approximate description of the initial nl populations, and small changes in the capture probabilities are needed to obtain agreement with experimental x-ray spectra. Our determination of the initial nl populations agrees well with experiment for $Ne^{10+}+He$ for which recoil spectroscopy data on selective level populations exist [26].

We present in Figs. 2(a)–2(d) the theoretical spectra degraded to a resolution of 50 eV. The individual lines of which the spectra are composed are identified in Table I. The higher energy peak in each spectrum consists primarily of the Lyman $6p$-$1s$ and $3p$-$1s$ lines of Ne^{9+} and the lower energy peak consists primarily of the Lyman $2p$-$1s$ line. The analysis yields accurate intensities of the many lines that appear at longer wavelengths in the radiative cascade from the initially populated levels. We list in Table I the predicted intensities scaled to the intensity of the Lyman α line of Ne^{9+}. There are several strong lines. The most prominent is the emission of the $3d$-$2p$ Balmer line at 189 eV for all targets. The relative intensities of the brightest emission lines are sensitive to the ionization potential of the target atoms and molecules. The point at 510 eV in the figures gives the total intensity of the $2s\rightarrow 1s$ two-photon decay continuum. Other possible sources of continuum emission are bremsstrahlung and radiative electron capture. Observation of the lines in Table I would provide a unique check on the electron capture hypothesis and a more accurate representation of the capture process [52]. Small but significant discrepancies exist between the experimental and model spectra on the low energy side of the major peaks. They may well be due to our neglect of multiple electron captures [23,26].

The derived initial populations are listed in Table II. They

TABLE II. Population of excited states of Ne^{*9+} ions.

Collision	n	ns	np	nd	nf	ng	nh	ni
$Ne^{10+}+He$	4	0.042	0.075	0.126	0.064			
	5	0.024	0.082	0.180	0.179	0.225		
	3	0.0	0.055	0.0				
$Ne^{10+}+H_2$	4	0.0	0.035	0.0	0.0			
	5	0.001	0.002	0.003	0.004	0.005		
	6	0.027	0.052	0.137	0.191	0.247	0.241	
	3	0.0	0.038	0.0				
$Ne^{10+}+H_2O$	4	0.0	0.028	0.0	0.0			
	6	0.027	0.025	0.10	0.12	0.16	0.12	
	7	0.008	0.024	0.04	0.057	0.083	0.089	0.07
	3	0.0	0.05	0.00				
$Ne^{10+}+CO_2$	5	0.024	0.0	0.032	0.0	0.0		
	6	0.047	0.031	0.16	0.19	0.22	0.21	
	7	0.0	0.001	0.002	0.003	0.004	0.005	0.003

are similar to those we obtained using the multicrossing Landau-Zener model and by molecular and classical-trajectory Monte Carlo calculations [33,34,51]. The values for H_2O should be particularly useful for the interpretation of cometary data.

We are grateful to P. Beiersdorfer and J. B. Greenwood for providing numerical data for their x-ray spectra. This work was partly supported by the National Aeronautics and Space Administration under Grant No. NAG5-4986.

[1] C.M. Lisse *et al.*, Science **274**, 205 (1996).
[2] V.A. Krasnopolsky *et al.*, Science **277**, 1488 (1997).
[3] K. Dennerl, J. Englhauser, and J. Trümper, Science **277**, 1625 (1997).
[4] M.J. Mumma, V.A. Krasnopolsky, and M.J. Abbott, Astrophys. J. Lett. **491**, L125 (1997).
[5] A. Owens *et al.*, Astrophys. J. Lett. **493**, L47 (1998).
[6] V.A. Krasnopolsky, M.J. Mumma, and M.J. Abbott, Icarus **146**, 152 (1998).
[7] C.M. Lisse *et al.*, Earth, Moon, Planets **77**, 283 (1999).
[8] C.M. Lisse *et al.*, Icarus **147**, 376 (1999).
[9] V.A. Krasnopolsky and M.J. Mumma, Astrophys. J. **549**, 629 (2001).
[10] C.M. Lisse *et al.*, Science **292**, 1249 (2001).
[11] R. Bingham *et al.*, Science **271**, 49 (1997).
[12] R. Bingham *et al.*, Astrophys. J., Suppl. Ser. **127**, 233 (2000).
[13] V. Krasnopolsky, Icarus **188**, 368 (1997).
[14] T.E. Cravens, Geophys. Res. Lett. **24**, 105 (1997).
[15] R.M. Häberli *et al.*, Science **276**, 939 (1997).
[16] R. Wegmann *et al.*, Planet. Space Sci. **46**, 603 (1998).
[17] N.A. Schwadron and T.E. Cravens, Astrophys. J. **544**, 558 (2000).
[18] V. Kharchenko and A. Dalgarno, J. Geophys. Res., [Space Phys.] **105**, 18 351 (2000).
[19] V. Kharchenko and A. Dalgarno, Astrophys. J. Lett. **554**, L99 (2001).
[20] J.B. Greenwood *et al.*, Astrophys. J. Lett. **533**, L175 (2000).
[21] P. Beiersdorfer *et al.*, Phys. Rev. Lett. **85**, 5090 (2000).
[22] G. Lubinski *et al.*, Phys. Rev. Lett. **86**, 616 (2001).
[23] J.B. Greenwood *et al.*, Phys. Rev. A **63**, 062707 (2001).
[24] P. Beiersdorfer *et al.*, Astrophys. J. Lett. **549**, L147 (2001).
[25] X. Ma *et al.*, Phys. Rev. A **64**, 012704 (2001).
[26] X. Flechard *et al.*, J. Phys. B **34**, 2759 (2001).
[27] A.A. Hasan *et al.*, Astrophys. J. Lett. **560**, L201 (2001).
[28] R.E. Olson, J. Phys. B **13**, 483 (1980).
[29] R.E. Olson and R. Schulz, Phys. Scr. **428**, 91 (1989).
[30] R.E. Janev and H. Winter, Phys. Rep. **117**, 265 (1985); *Atomic and Molecular Processes in Fusion Edge Plasmas*, edited by R. E. Janev (Plenum, New York, 1995).
[31] A. Kumar and B.C. Saha, J. Phys. B **31**, L937 (1998).
[32] C. Harel and A. Jouin, J. Phys. B **25**, 221 (1992).
[33] C. Harel *et al.*, At. Data Nucl. Data Tables **68**, 279 (1998).
[34] P. Stancil *et al.*, J. Phys. B **34**, 1 (2001).
[35] M. Ishimoto *et al.*, J. Geophys. Res., [Space Phys.] **91**, 5793 (1986).
[36] E.C. Roelof, Geophys. Res. Lett. **14**, 652 (1987).
[37] A.E. Metzger *et al.*, J. Geophys. Res., [Space Phys.] **88**, 7731 (1983).
[38] J.H. Waite *et al.*, J. Geophys. Res., [Space Phys.] **99**, 14 799 (1994).
[39] T.E. Cravens *et al.*, J. Geophys. Res., [Space Phys.] **100**, 17 153 (1995).
[40] V. Kharchenko, W. Liu, and A. Dalgarno, J. Geophys. Res., [Space Phys.] **103**, 26 687 (1998).
[41] T.E. Cravens, Astrophys. J. Lett. **532**, L153 (2000).
[42] T.E. Cravens, I.P. Robertson, and S.L. Snowden, J. Geophys. Res., [Space Phys.] **106**, 24883 (2001).
[43] H. Bloemen *et al.*, Astron. Astrophys. **281**, L5 (1994).
[44] V. Tatischeff *et al.*, Astrophys. J. **504**, 874 (1998).
[45] E. Källne *et al.*, Phys. Rev. Lett. **52**, 2245 (1984).
[46] G.J. Ferland *et al.*, Astrophys. J. Lett. **481**, L115 (1997).
[47] T. Cho *et al.*, Phys. Rev. Lett. **64**, 1373 (1990).
[48] B.J. Wargelin and J.J. Drake, Astrophys. J. Lett. **546**, L57 (2001).
[49] I.I. Sobelman, *Atomic Spectra and Radiative Transitions* (Springer, Berlin, 1996).
[50] D. Huang-Binh, Astron. Astrophys. **238**, 449 (1990).
[51] J.A. Perez, R.E. Olson, and P. Beiersdorfer, J. Phys. B **34**, 3063 (2001).
[52] M. Suraud *et al.*, J. Phys. B **24**, 2543 (1991).